ISSN 2616-5767 Vol.8, Issue 5: 93-100, DOI: 10.25236/AJETS.2025.080513

Analysis of Impact Response Characteristics of Typical Gas Turbine Components

Pengwei Lv[1,a], Fulin Yu[1,*]

[1]School of Naval Architecture and Port Engineering, Shandong Jiao Tong University, Weihai, Shandong, 264209, China
[a]lpw18365648260@163.com
**Corresponding author: yufulin@sdjtu.edu.cn*

Abstract: *In order to investigate the response characteristics of gas turbines under impact loads, an equivalent finite element model of the gas turbine was established in Abaqus, with a focus on refining the mesh of the support legs and key connection parts. The impact loads were converted into positive and negative combined triangular wave inputs according to the BV043/85 standard. Subsequently, calculate the impact response of the structure and extract the acceleration time history data of the bottom, middle, and top of the support legs. Finally, the HHT method improved by CEEMDAN was used to analyze the acceleration signal and obtain the distribution pattern of the impact response in the support legs. The results indicate that the impact stress gradually attenuates during the structural transmission process and mainly concentrates at the structural connections and the edges of the support legs; On a rigid installation foundation, the acceleration response exhibits significant high-frequency components, and as energy is transferred within the structure, the proportion of high-frequency component energy gradually decreases; There are spatial differences in the acceleration energy distribution of different legs, and the proportion of high-frequency components in the rear leg is generally higher than that in the front leg.*

Keywords: *Gas turbine; Impact response; Transmission characteristics; Time-frequency analysis*

1. Introduction

During the service process, ships will inevitably face various severe explosion impact environments. The underwater explosion they suffer mainly includes contact explosion and non-contact explosion. The strong load generated by non-contact underwater explosion is the main threat source, and the huge impact load imposed instantaneously can be transferred to internal equipment through the hull structure[1-3]; Although civilian ships are less likely to encounter explosive impacts, they may still experience unexpected events such as slamming, grounding, and collisions under harsh sea conditions, resulting in strong transient impact loads. These impact loads have the characteristics of high peak value, short duration, and wide frequency range, which can easily lead to serious consequences such as plastic deformation of the structure, loosening or fracture of key connectors, damage to shaft alignment, and even overall equipment failure. As one of the core components of ship power systems, gas turbines have complex and precise structures, including numerous moving parts and ancillary systems. Under the impact load, the equipment faces severe challenges such as structural integrity risk, failure of moving parts, damage to ancillary systems, and loss of function. Traditional impact resistance research heavily relies on physical impact tests (such as impact test benches, underwater explosions of real ships, etc.). Although the test results are intuitive and reliable, they have significant disadvantages such as extremely high cost, long cycle, strong destructiveness, low repeatability, and difficulty in covering all working conditions[1]. Therefore, numerical analysis can be carried out by establishing equivalent mechanical models to deepen mechanism research while reducing research and development costs and risks, focusing on analyzing the transmission path of impact energy inside complex structures, the dynamic response characteristics of key components, and potential weak links.

In the field of shock resistance in gas turbines, research focuses on structural and strength design[4,5], while there is relatively little research on the propagation mechanism of impact loads in structures[6]. When studying the transmission characteristics of loads in structures and spectral analysis, the main methods are Fourier spectrum and shock response spectrum[7,8]. At the same time, for the non-stationary nature of underwater explosion shock wave signals, the Hilbert Huang Transform(HHT) can be selected

ISSN 2616-5767 Vol.8, Issue 5: 93-100, DOI: 10.25236/AJETS.2025.080513

for time-frequency analysis of shock response. The Complete Ensemble Empirical Mode Decomposition with Adaptive Noise(CEEMDAN) has strong adaptability and can effectively suppress mode mixing, thereby obtaining high-precision Hilbert spectrum and marginal spectrum[9]. Xiong Banghu[10] established an equivalent mechanical model for gas turbines and conducted time-frequency analysis of response signals using an improved HHT method. It was found that the proportion of high-frequency energy along the propagation path of the shock wave in the gas turbine decreases with the increase of load transmission distance, corresponding to the stress response of the gas turbine. Zhou Peng[11] used an improved HHT method to compare the distribution and transmission characteristics of impact loads in different directions between single hull and three body ships, and obtained the relationship between different frequency components and shock response, verifying the effectiveness of the HHT method in studying load distribution and transmission characteristics.

Therefore, this paper established an equivalent mechanical model for gas turbines, calculated impact loads in the finite element software Abaqus, and used CEEMDAN-Hilbert method for time-frequency analysis of shock response to study the response distribution and transmission characteristics of gas turbines under typical shock loads.

2. Finite Element Model and Operating Condition Setting

2.1. Finite Element Model

This paper studies the impact response and transmission law of the support legs and key connections of a gas turbine under impact loads. The impact platform is located at the bottom of the gas turbine, with a rigid installation foundation and a vertical impact direction. Equivalent modeling is performed on the rotor and casing parts, and more detailed mesh division is carried out on the support legs and the transmission path of the response in front of the support legs. A finite element model is established in Abaqus as shown in Fig. 1, with a size of 2.5 m × 2 m × 3 m for the gas turbine.

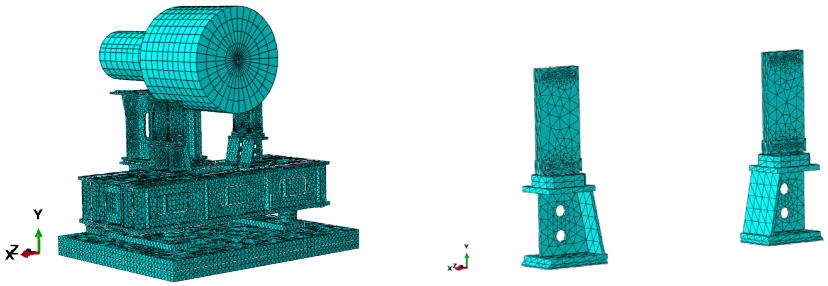

Figure 1: Finite Element Model and Leg Structure of Gas Turbine.

2.2. Impact load input

In the German ship impact resistance standard BV043/85, the impact resistance indicators are divided into three categories according to the installation location of the equipment, as shown in Tab. 1. Among them, Class I installation locations refer to the ship's outer panels or outer panel reinforcements, double-layer bottom and top panels, and bulkheads below the main deck; Class II installation locations refer to the lower deck and main deck, adjacent walls below the main deck, and bulkheads above the main deck; Class III installation locations refer to the deck above the main deck, the side partition above the main deck, and the middle partition[12].

Table 1: Partial impact environment of BV043/85[12].

Location	Direction	D_0(cm)	V_0(m/s)	A_0(g)
I	Vertical	4.3	7.0	320
	Horizontal	3.0	6.0	280
II	Vertical	4.2	6.0	170
	Horizontal	3.0	3.1	100
III	Vertical	5.2	5.0	100
	Horizontal	4.7	3.0	30

For equipment with a mass greater than 5 t, spectral velocity and spectral acceleration need to be

ISSN 2616-5767 Vol.8, Issue 5: 93-100, DOI: 10.25236/AJETS.2025.080513

reduced:

$$(\frac{A}{A_0}) = (\frac{m}{m_0})^{-0.537}, (\frac{V}{V_0}) = (\frac{m}{m_0})^{-0.4} \tag{1}$$

Among them, A is the reduced spectral acceleration; V is the reduced spectral velocity; m is the quality of the isolated installation equipment; m_0 is the mass constant, which remains constant at 5 t.

The BV043/85 standard states that converting shock loads into positive and negative combinations of triangular wave shock signals results in triangular wave pulses that are closer to the underwater explosion shock spectrum and are easier to input as boundary conditions in calculations. Therefore, in simulation calculations, the acceleration time history of positive and negative combinations of triangular waves is usually used, as shown in Fig. 2, which is the acceleration time history curve composed of high amplitude positive pulses with smaller time scales and low amplitude negative pulses with larger time scales.

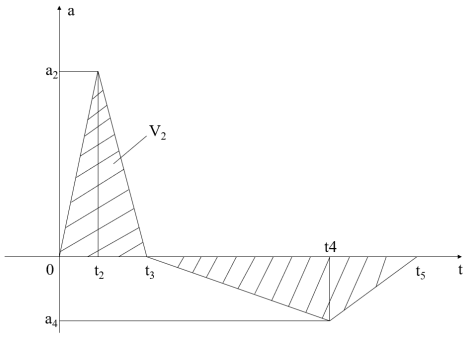

Figure 2: Combined triangular wave load.

The peak value of positive pulse acceleration a_2 is about 0.6 times the maximum acceleration; The positive and negative pulse areas are equal, with a magnitude of approximately 0.75 times the maximum velocity; For time t, $t_2 = 0.4t_3$ and $t_4 - t_3 = 0.6(t_5 - t_3)$ are satisfied; The displacement obtained by integrating the acceleration twice is 1.05 times the maximum relative displacement in the design spectrum. Namely:

$$a_2 = 0.6A_{\max}, S_1 = 0.75V_{\max}, t_3 = \frac{2v_1}{a_2}, t_2 = 0.4t_3 \tag{2}$$

$$t_5 = \frac{6.3D_s}{1.6a_2t_3}, a_4 = -\frac{a_2t_3}{t_5 - t_3}, t_4 = t_3 + 0.6(t_5 - t_3) \tag{3}$$

After calculation, the parameters of the triangular wave of the gas turbine impact load are shown in Tab. 2:

Table 2: Combined triangular wave load parameters.

Parameters	vertical
a_2(g)	192.0
a_4(g)	-101.6
t_2(s)	0.00223
t_3(s)	0.00558
t_4(s)	0.01195
t_5(s)	0.0162

3. CEEMDAN Hilbert Transform

Underwater explosion signals have characteristics such as non stationarity, short time, fast mutation, and wide frequency band. In signal processing, it is crucial to analyze the frequency components of the signal and their relationship with time variation. Although the traditional Fourier transform method has

ISSN 2616-5767 Vol.8, Issue 5: 93-100, DOI: 10.25236/AJETS.2025.080513

powerful functions in frequency domain analysis, it cannot provide the frequency characteristics of signals at any time, so it is not suitable for the analysis of non-stationary signals. To overcome the limitation of Fourier transform, it is necessary to perform time-frequency analysis on the signal.

HHT transform is an adaptive time-frequency analysis method used to analyze nonlinear and non-stationary signals. Unlike traditional methods such as Fourier transform, HHT does not rely on prior basis functions. Instead, based on the local characteristics of the signal itself, it transforms complex non-stationary signals into a superposition of simple intrinsic mode functions through empirical mode decomposition, and then performs Hilbert spectral analysis on the intrinsic mode functions.

3.1. CEEMDAN

Empirical Mode Decomposition(EMD) is the key to HHT transformation, which decomposes a complex signal $x(t)$ into multiple Intrinsic Mode Function(IMF) components with a single frequency feature, which can better reflect the local characteristics and dynamic changes of the signal. Namely:

$$x(t) = \sum_{i=1}^{n} IMF_i(t) + r_n(t) \tag{4}$$

In the formula, $IMF_i(t)$ is the intrinsic modal component and $r_n(t)$ is the residual signal.

The specific steps of EMD are: 1) Identify all extreme points of $x(t)$, use cubic spline interpolation to fit the upper and lower envelope lines, and calculate the mean envelope line $m_1(t)$; 2) Subtract the mean envelope line from the original signal to obtain $IMF_1(t)$, and subtract $IMF_1(t)$ from the original signal to obtain the residual component $r_1(t)$; 3) Repeat the above steps for the residual components to obtain new IMF components and residual components.

The IMF component must meet the termination criteria, which means that the difference between the number of extreme points and the number of zero crossings should not exceed 1, and the mean of the upper and lower envelope lines must be zero or close to zero at any time point.

To solve the mode mixing problem in EMD, CEEMDAN adds different Gaussian white noise based on the characteristics of the original signal, repeats multiple times, and obtains multiple different synthesized signals:

$$y_n(t) = x(t) + \varepsilon z_n(t) \tag{5}$$

In the equation, ε is the standard deviation of Gaussian white noise.

On this basis, these synthesized signals are subjected to empirical mode decomposition, and the components obtained are averaged to obtain $IMF_1(t)$. The residual signal is obtained by subtracting the original signal from $IMF_1(t)$. Gaussian white noise is added to the residual signal and the above steps are repeated to obtain new IMF components and residual components until the residual signal becomes a monotonic signal.

Compared to EMD, CEEMDAN is an advanced signal processing technique that effectively solves the mode mixing problem in EMD by introducing adaptive noise and multiple iterations. It also improves the problem of white noise in IMF caused by Ensemble Empirical Mode Decomposition(EEMD) and Complete Ensemble Empirical Mode Decomposition(CEEMD), and enhances the accuracy and stability of decomposition.

3.2. Hilbert transform

Hilbert transform is defined as the convolution of the original function with $h(t) = \frac{1}{\pi t}$:

$$x_h(t) = pv\int_{-\infty}^{\infty} x(\tau)\frac{1}{\pi(t-\tau)}d\tau \tag{6}$$

In the equation, p and v are Cauchy principal values.

Using the original signal as the real part and Hilbert transform as the imaginary part, an analytical

ISSN 2616-5767 Vol.8, Issue 5: 93-100, DOI: 10.25236/AJETS.2025.080513

function can be constructed:

$$X(t) = x(t) + jx_h(t) \tag{7}$$

The instantaneous amplitude, frequency, and phase of the original signal can be obtained through analytical functions:

$$A(t) = \sqrt{x(t)^2 + x_h(t)^2} \tag{8}$$

$$\varphi(t) = \arctan\frac{x_h(t)}{x(t)} \tag{9}$$

$$f(t) = \frac{d\varphi(t)}{dt} \tag{10}$$

The Hilbert spectrum $H(\omega,t)$ can be obtained by superimposing the instantaneous amplitude and frequency of all IMF components. Integrating the Hilbert spectrum timeline yields the marginal spectrum $h(\omega)$ of the signal. The Hilbert spectrum provides information on the instantaneous changes in time and frequency of the signal, while the marginal spectrum reflects the energy distribution of the signal at different frequencies.

4. Time-frequency analysis of impulse response

The stress response of the gas turbine under vertical impact load is shown in Fig. 3. The stress concentration area mainly occurs in the bottom of support leg and the connection with the fan, with the maximum value appearing at the top of the support leg and the connection with the fan. The overall stress distribution is uniform, and there is no large-scale stress concentration.

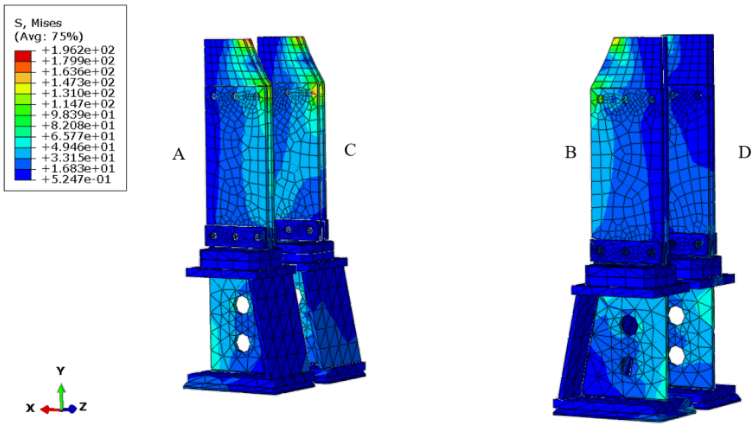

Figure 3: Stress cloud picture of gas turbine leg structure.

Measurement points were set at the stress concentration positions at the top, middle, and bottom of the support leg, and the acceleration response time history data were extracted. The acceleration time history data at the bottom, middle, and top of support leg A are shown in Fig. 4. On the basis of rigid installation, the acceleration response of each measuring point exhibits obvious high-frequency oscillation and transient impact characteristics[13]. From the acceleration time history, it can be seen that in the initial stage of response, the acceleration amplitude is high and the high-frequency oscillation is small. As the load action time increases, the high-frequency oscillation in the response gradually increases. At the same time, from the bottom of the support leg to the top, both the initial response amplitude and high-frequency oscillation amplitude show a decreasing trend. This is because the gas turbine structure results in the gradual decay of the impact load energy during the transmission process.

ISSN 2616-5767 Vol.8, Issue 5: 93-100, DOI: 10.25236/AJETS.2025.080513

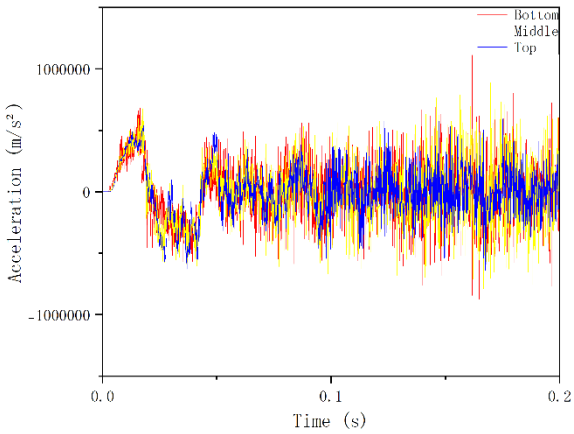

Figure 4: Acceleration response time history of leg A.

To further investigate the dynamic response characteristics of the leg structure under impact loads, this paper uses the CEEMDAN method to decompose the acceleration time history signal of the bottom measurement point of leg A. As an improved algorithm of EMD, CEEMDAN effectively suppresses the mode mixing problem in traditional EMD methods by adding adaptive white noise multiple times and taking the average value, significantly improving the accuracy and effectiveness of decomposition.

During the decomposition process, the noise standard deviation is 0.2 and the average number of iterations is 50. The original signal is decomposed into 10 IMFs and one residual. As shown in Fig. 5, from IMF1 to IMF10, the frequency gradually decreases, the wavelength gradually increases, and the amplitude generally shows a decreasing trend, fully covering the wideband range from high frequency to low frequency, presenting typical multi-scale signal decomposition characteristics.

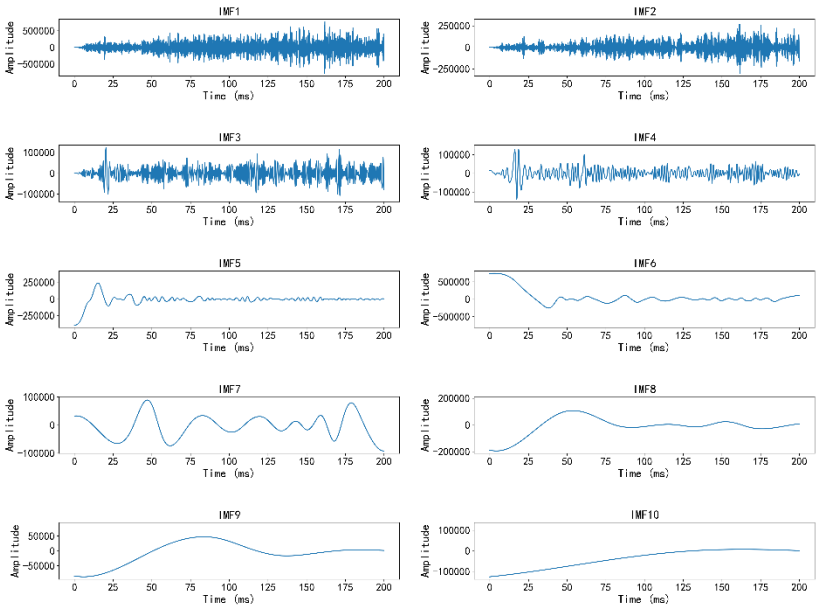

Figure 5: IMFs of lower acceleration response of leg A.

Perform Hilbert transform on all IMFs, construct analytical functions, calculate instantaneous amplitude and frequency, and obtain Hilbert spectra, as shown in Fig. 6. In the initial response stage, the amplitude of the acceleration response is high while the frequency is low. In the first period, approximately 50ms, the energy is mainly distributed below 250 Hz, and then obvious high-frequency oscillations begin to appear. At the same time, instantaneous high amplitude appear during the oscillation process, and the frequency and amplitude of the signal show complex distribution characteristics over time. By integrating the Hilbert spectrum along the time axis, the marginal spectrum of the signal can be obtained, as shown in Fig. 7. After time scale accumulation, the high amplitude mainly appears in the low frequency part, and although the high frequency part also has high amplitude, it generally has a short duration and a wide overall frequency band range. Therefore, it exhibits a distribution characteristic of low amplitude scale and wide frequency scale in the marginal spectrum.

ISSN 2616-5767 Vol.8, Issue 5: 93-100, DOI: 10.25236/AJETS.2025.080513

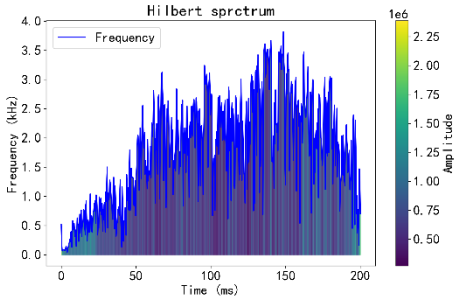

Figure 6: Hilbert spectrum of acceleration response at the bottom of leg A.

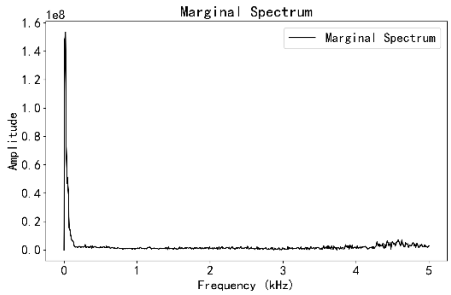

Figure 7: Marginal spectrum of acceleration response at the bottom of leg A.

Using the same method, the time history marginal spectra of acceleration in the middle and top of leg A were obtained, as shown in Fig. 8. Comparing the marginal spectra of different parts, it can be seen that from the bottom to the top of the leg, the maximum amplitude decreases, while the frequency distribution range in the low-frequency range increases.

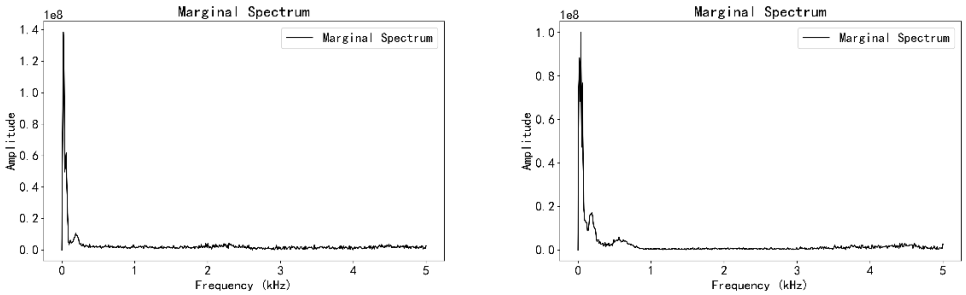

Figure 8: Marginal spectrum of acceleration response in the middle and top of leg A.

In the frequency domain, using 250 Hz as the standard, frequency above 250 Hz are referred to as high frequency, and frequency below 250 Hz are referred to as low frequency[14]. To conduct a detailed analysis of the frequency domain distribution characteristics of the impact response at each measuring point, the energy proportion of the acceleration time history signals at all measuring points was statistically analyzed. The results are shown in tab. 3, and there is a significant spatial pattern in the energy distribution of the acceleration response. From the bottom to the top, all leg responses exhibit a decreasing high-frequency response, and from the middle to the top, high-frequency components are significantly attenuated, which is related to the flexible support structure in the middle of each leg. At the same time, there are certain differences in the energy distribution of the acceleration response of the front and rear legs, with a higher proportion of high-frequency components in the response of the rear leg, which is related to the differences in energy transmission paths and uneven spatial distribution of structural stiffness and damping.

Table 3: Statistics of energy proportion at different positions of gas turbine leg structure.

	A		B		C		D	
	Low	High	Low	High	Low	High	Low	High
Bottom	38.99	61.01	34.21	65.79	28.45	71.55	30.68	69.32
Middle	43.05	56.95	42.45	57.55	35.26	64.74	34.68	65.32
Top	76.92	23.08	69.11	30.89	53.80	46.20	52.87	47.13

ISSN 2616-5767 Vol.8, Issue 5: 93-100, DOI: 10.25236/AJETS.2025.080513

5. Conclusions

This paper established an equivalent finite element model of a gas turbine, converts the impact load into a combined triangular wave signal, and combines the improved HHT method to conduct time-frequency analysis of the impact response characteristics of the gas turbine. The following conclusions are drawn:

(1) The load first acted on the bottom plate, is transmitted to the base through the impact platform, and finally reaches the support legs. During the transmission process, stress is mainly concentrated at the structural connections and the edges of the support legs. Under the combined triangular wave load, the maximum stress is reached at the bottom of the support legs after about 20ms, and the stress begins to decrease after 24ms.

(2) On the basis of rigid installation, there are significant high-frequency components in the acceleration response, and the overall amplitude of the front leg is higher than that of the rear leg, indicating that the overall vibration intensity of the front leg is greater and experiences stronger dynamic response.

(3) In acceleration response, high frequency is the main dominant component, and as energy is transferred, the proportion of high frequency components gradually decreases; At the same time, there is a certain difference in the energy distribution of the acceleration response of the supporting legs, with the high-frequency component of the rear supporting leg accounting for a higher proportion than that of the front supporting leg.

References

[1] Zhang, A. M., Ming, F. R., Liu, Y. L., et al. A review of underwater explosion load characteristics and research on ship damage and protection under such loads[J]. Chinese Journal of Ship Research, 2023, 18(3), 139–154, 196.
[2] Haopeng G, Hengdou T, Xiaotong G. Damage characteristics of cabin in navigational state subjected to near-field underwater explosion[J]. Ocean Engineering, 2023, 277.
[3] Nagesh, K. N G. Underwater Explosion (UNDEX) Phenomenon and Response of Marine Combatants to UNDEX Loading[J]. Mechanics of Solids, 2023, 58(1): 338-351.
[4] ZHAO S T, WANG N, WANG X, et al. Numerical study on dynamic Response of ship structure and gas turbine under underwater explosion[J]. Journal of Ship Mechanics, 2021, 25(6): 815-827.
[5] Meng, C., Fan, K., Cai, B. W. Simulation and optimization of ejector efficiency of gas turbine exhaust pipe[J]. Ship Science and Technology, 2022, 44(7), 113–117.
[6] Yao, X. L., Xiong, B. H., Wang, Z. K., et al. Transmission characteristics of underwater explosion shock wave load along gas turbine structure[J]. Acta Armamentarii, 2022, 43(9), 2367–2378.
[7] Wang, S. Study on the characterization method of impact load on marine gas turbine components[D]. Harbin Engineering University, 2022.
[8] Li, Y. J., Chen, X., Zeng, Q. P., et al. Review of ship power equipment impact resistance assessment methods[J]. Chinese Journal of Ship Research, 2024, 19(3), 61–85.
[9] Fan, T., Wang, X. N., Wu, Y., et al.. Research on time-frequency analysis method of underwater explosion signal based on CEEMDAN-Hilbert transform[J]. Journal of Shenyang Ligong University, 2024, 43(5), 20–26.
[10] Xiong, B. H. Research on transient strong impact analysis method and response characteristics of ship-borne gas turbine components[D]. Harbin Engineering University, 2023.
[11] Zhou, P. Analysis of underwater explosion load transmission and impact environment characteristics of trimaran[D]. Harbin Engineering University, 2020.
[12] Liu, J. H., Pan, J. Q., He, B. Comparison of impact resistance standards for equipment in major naval countries[J]. Applied Science and Technology, 2010, 37(9), 17–25.
[13] Shi, S. H., Feng, L. H., Du, Z. P., et al. Analysis of influencing factors on impact resistance design indexes of elastically isolated installed equipment[J]. Chinese Journal of Ship Research, 2019, 14(1), 66–71.
[14] Wang, J. Study on impact dynamic characteristics of floating impact platform[D]. Harbin Engineering University, 2015.